ELSEVIER

Journal of Neuroscience Methods 106 (2001) 121–129

JOURNAL OF NEUROSCIENCE METHODS

www.elsevier.com/locate/jneumeth

# A simple method to microinject solid neural tracers into deep structures of the brain

Gonzalo Marín [a], Pablo Henny [a], Juan Carlos Letelier [a], Elisa Sentis [a], Harvey Karten [b], Bruce Mrosko [b], Jorge Mpodozis [a,*]

[a] *Departamento de Biología, Universidad de Chile, Casilla 653, Santiago, Chile*
[b] *Department of Neurosciences, School of Medicine, University of California, San Diego, CA, USA*

Received 1 November 2000; received in revised form 10 January 2001; accepted 10 January 2001

**Abstract**

We have developed an instrument to perform microinjections of solid neural tracers into deep structures of the brain. The instrument consists of a thin hypodermic needle equipped with a movable internal rod, which is connected to a pressure chamber. When a pressure pulse is applied to the chamber, the rod moves forward and back inside the needle, pushing out a solid load previously packed inside the needle tip. By attaching a microelectrode to the instrument, it is also possible to have electrophysiological control of the injection placement. To test the instrument, we microinjected DiI and rhodamine crystals into selected structures of the visual system of pigeons. The results show small, well-defined injection sites, accurately located in the desired targets, together with well-developed anterogade and retrograde transport, selectively originated from the injection sites. This method extends the usage of solid tracers to most structures in the brain and may, in certain cases, be more advantageous than the conventional method of injecting tracer solutions. 

*Keywords:* Neuronal tracing; Microinjections; DiI; Thalamus; Visual system; Birds

## 1. Introduction

Neural tracers are frequently applied in their crystalline form (Griffin et al., 1979; Escher et al., 1983; Dietrichs and Walberg, 1986; Keller et al., 1986; Köbbert et al., 2000). Compared to injections of dissolved tracers, this procedure has the advantage of producing a very steep concentration gradient of the tracer around the crystal, enhancing the labeling efficiency of the tracer and reducing its diffusion. The introduction of fluorescent dyes, especially the lipophilic carbocyanine dyes, have favored the use of crystalline deposits of tracers in a variety of studies, from neural connectivity and its development to axonal pathfinding and neural cell migration (Catsicas et al., 1987; Thanos and Bonhoefer, 1987; Nakamura and O'Leary, 1989; Tamamaki et al., 1997; Köbbert et al., 2000).

The common method used to insert crystalline tracers has been by means of small forceps or other sharp instruments controlled by hand, thus restricting this method's use mostly to accessible structures like the retina (Thanos and Bonhoefer, 1983; Catsicas et al., 1987; Nakamura and O'Leary, 1989), the optic nerve (Thanos et al., 1994), the spinal cord (Griffin et al., 1979) or peripheral nerves (Cruz et al., 1987; Novikova et al., 1997). The injection of crystalline tracers into deep structures has proven to be more difficult, and the procedures implemented (Dietrichs and Walberg, 1986; Bechmann and Nitsch, 1997; Tamamaki et al., 1997) do not permit easy control of the position or the size of the injection.

In this paper, we report a simple method to accurately inject a small cylindrical pellet of crystalline tracer of a predetermined size into any structure of the brain that can be reached stereotaxically. The method is based on a specially-designed, pressure-driven 'Solid Microinjector'. To illustrate its application, we injected crystals of DiI and rhodamine-isothiocyanate (RITC) into three structures of the pigeon visual system: the

* Corresponding author. Tel.: +56-2-6787235; fax: +56-2-2712983.
*E-mail address:* epistemo@uchile.cl (J. Mpodozis).

0165-0270/01/$ - see front matter 
PII: S0165-0270(01)00332-6

nucleus rotundus, the ventral nucleus of the lateral geniculate and the retina.

## 2. Methods

### 2.1. The solid microinjector

The solid microinjector apparatus consists of three main components: a thin, blunt 30 g hypodermic needle, an internal stainless steel rod that fits the inner diameter of the needle, and a syringe-like pressure chamber (Fig. 1A). When a gas pressure pulse is applied to the chamber, the rod moves forward and back inside the needle, pushing out a solid load that has been previously packed internally in the needle tip.

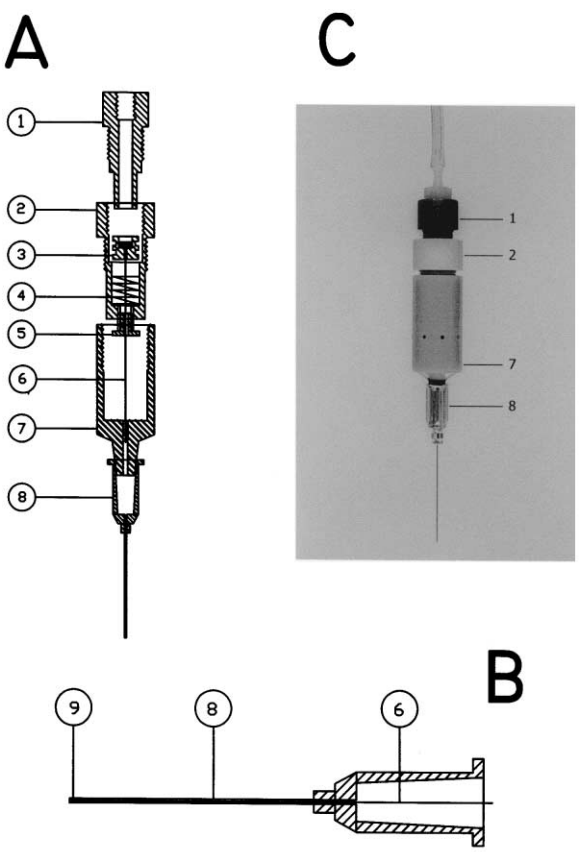


Fig. 1. The solid microinjector: (A) Schematic drawing of the instrument showing the arrangement of the different parts: upper body (1), central body (2), piston (3), spring (4), bushing (5), rod (6), lower body (7), and hypodermic needle (8); (B) Detailed drawing of the instrument tip showing how the crystal (9) is loaded in the space left by the rod (6) inside the needle (8); (C) Photograph of the assembled microinjector. A piece of tubing, to convey the pressure pulses, and a threaded fit connecting the tubing to the upper body are also displayed. Note the ring of small perforations in the bottom half of the lower body, designed to release the excess pressure (Section 2). All the machined parts are custom-made and can be produced in a professional machine shop. The drawings are to scale. The needle length is 39 mm in all illustrations.

The pressure chamber is composed of three independent, hollow cylindrical bodies screwed serially one inside the other. The upper body is screwed to the inner wall of the central body that, in turn, is screwed to the inner wall of the lower body. The thread in each body is machined for a tight fit, so the three parts, when assembled, produce a rigid and stable unit. The central body contains a short spring, on top of which is seated a plastic piston, which smoothly fits the inner diameter of the bottom half of this body. The rod is perpendicularly attached to the center of the piston by means of a tubular metal bracket. The bottom of the central body has a small bushing through which the rod moves. The lower body is shaped like the bottom half of a syringe with a tip that holds the needle. This tip has a thin central perforation that allows the passage of the rod into the needle. The upper body is opened on both ends. The superior opening is connected to the pressure source, by means of a threaded fit, while the inferior opening fits inside the central body, immediately on top of the piston, serving as a stop end for the piston movement.

When a positive pressure pulse is applied to the chamber, the piston in the central body pushes down the spring and produces a forward movement of the rod inside the needle. When the pressure pulse ends, the spring pushes the piston up, restoring the rod to its resting position. The excursion of this movement can be regulated by screwing the upper body upwards or downwards with respect to the central body. Similarly, the resting position of the rod inside the needle can be adjusted by screwing the central body upwards or downwards with respect to the lower body. Finally, excess pressure is released by means of a series of small perforations made around the perimeter of the lower and central bodies.

### 2.2. Materials

The upper body is made of Ultem 1000. This material provides shock resistance and excellent dielectric properties. The central body is composed of Techtron Polyphenylene Sulfide. This material possesses high stress and tensile strength for a precise-tolerance machined component. The lower body is composed of 30% glass Ultem 2300, which provides a high dielectric medium and ultimate rigidity. The piston is made of Vespel, which allows for precision machining and provides the smooth surface finish required to obtain freedom of movement. The drive rod is composed of 304 V stainless steel, for high strength and alignment properties. The spring is made of thin 18–8 stainless steel wire.

### 2.3. Loading the microinjector and calibrating the injection parameters

The microinjector can easily be loaded by pushing the tip of the needle gently against the crystals, until a compressed pellet of the crystal fills the space left by the retracted rod inside the needle tip (Fig. 1B). The loading operation can be done manually with the aid of a low-power microscope. When a water soluble crystal, such as RITC, is used, the tip of the needle must be covered to prevent the dilution of the tracer as the tip is brought into contact with the tissue. A brief immersion of the tip in melted bone wax serves well for this purpose. The length of the cylindrical pellet can be set in the range of 50 to several hundred micrometers by adjusting the resting position of the rod inside the needle. The excursion of the rod out of the needle should be adjusted so as to push the load at least 100–200 μm away from the needle tip, otherwise the pellet may remain attached to the tip after the extrusion movement. To calibrate the excursion and the resting position of the rod, first the excursion of the rod is set (by rotating the upper body with respect to the central body), with the rod in an extruded position. This can be accomplished under a microscope with a calibrated grid, while repetitive pressure pulses are applied to the instrument. Then the rod is retracted (by rotating the central body with respect to the lower body) until its tip extrudes the desired amount during each pressure pulse. The distance the rod tip travels inside the needle corresponds to the space left for the load when the rod is in the resting position. A practical way to test the instrument is to load it with a colored crystal and to practice trial injections into a semisolid transparent medium, such as agar 3%.

### 2.4. The pressure pulses

An $N_2$ balloon at 1000 psi functioned as a pressure source. The pressure drive was a custom-made picospritzer device, coupled to a square-pulse generator (Grass S4 Stimulator). A commercial picospritzer apparatus (such as Picospritzer II, General Valve Corp.) can also be used. In our system, pulses of 50 psi were sufficient to produce rapid and strong movements of the rod, but this value may vary in a different system. To guarantee the complete ejection of the tracer, a train of 10 pulses (0.2 s duration at 1 Hz) was applied.

### 2.5. Recording attachment

In order to obtain electrophysiological identification of the structures to be injected, a tungsten microlectrode can be attached to the microinjector. To this end, the microelectrode is inserted through a short, thin 30-gauge metal tube that is glued to the exterior wall of the needle. With this arrangement, the electrode runs parallel to the needle, laterally displaced approximately 50 μ. Once the microinjector has been calibrated and loaded, the microelectrode is manually inserted through the guide. Under microscopic inspection, the tip of the electrode is located in the desired position with respect to the needle tip, and the electrode is secured to the needle with a small drop of fast-acting glue. The superior portion of the electrode is secured to the pressure chamber using a small clip.

### 2.6. Test experiments

Eight adult pigeons (*Columba livia*), 300–350 g body weight, of both sexes, were used in these experiments. Six of them received injections of DiI into the brain and two received injections of RITC into the retina. These animals were obtained from a local dealer and kept in an institutional animal-facility environment. All the experimental procedures were done in accordance with the guidelines of the Science Faculty's Ethics Committee (Comite de Etica de la Facultad de Ciencias de la Universidad de Chile).

The pigeons were deeply anesthetized with equithesin (0.3 ml × 100 g body weight supplemented by 0.2 ml every 2 h), and mounted, in the standard stereotaxic position (Karten and Hodos, 1967), in a specially designed head holder, which produces no visual field interference. For the brain injections, the top of the skull was exposed and a craniotomy was done above the approximate location of the structure to be injected. The microinjector, loaded and with a microelectrode attached, was held in a hydraulic microdrive and stereotaxically positioned and advanced to the selected target. For the retinal injections, a small opening near the eye equator was cut through the skin and underlying sclera, through which the tip of the microinjector was introduced. Electrophysiological signals were amplified (using a 1800 dual probe amplifier, AM Systems), displayed in an oscilloscope (Tektronix 5113) coupled to an audio monitor (Optimus SA-155), recorded in a video digital recorder (Instrutech VR-10B), fed to a PC computer provided with a D/A card (National Instrument) and sampled at 10 KHz using custom-made data acquisition routines (written in Lab View 3.0). Visual responses were elicited with a custom-made, computer-driven, visual stimulation system, composed of two slide projectors (Leitz Prado), two electro-mechanical shutters, a mirror mounted in a DC galvanometer (Grass Polygraph S-400), a series of interference and neutral filters (Ealing optics), and a dove prism, plus the necessary drivers and power sources. Once the target structures were electrophysiologically identified, the injection was made applying pressure pulses according to the parameters described above. After a settling period of 3–5 min, the microinjector

was slowly withdrawn, and the wound was covered, sutured and treated with topical antibiotics. During the experiment, the heart rate of the animals was continuously monitored and the body temperature was held at 42°C by means of a thermoregulated electric blanket. During surgery and recovery, all the wounds and pressure points were treated with a commercial ointment of 5% lidocaine.

After 5–20 days of survival, the animals were deeply anesthetized with an overdose of equithesin, and perfused via the aorta with 500–800 ml of avian ringer, followed by 1000 ml of a cold (10°C) solution of 4% paraformaldehyde in 0.1 M phosphate buffer (pH 7.2). After the perfusion, the brains and eyes were excised. The retinae and the attached choroid were separated from the sclera, air-dried, mounted with the ganglion cell layer upwards and photographed with a conventional camera. Brains were post-fixed overnight in paraformaldehyde solution and then transferred for 1 or 2 days to a 30% sucrose solution for cryoprotection. The brains were then mounted in the stereotaxic plane on the stage of a frozen sliding microtome, and cut into 45 μm sections. The sections were immediately mounted and coverslipped using a solution of 50% glycerol in avian saline. The sections were then examined and photographed for transmitted light and rhodamine fluorescence using a conventional epifluorescent microscope (Olympus B × 60) equipped with a digital camera and software (Spot Digital Camera, Diagnostic Instruments). Collected images were transferred into Adobe Photoshop 5.0 for final composition.

## 3. Results

### 3.1. DiI injections into the nucleus rotundus

The nucleus rotundus (Rt) is the thalamic relay of the ascending tectofugal pathway of birds. It receives a massive bilateral projection from cells of the main output layer of the optic tectum, layer 13, and projects almost exclusively to the ipsilateral ectostriatum (Benowitz and Karten, 1976). It also receives strong ipsilateral gabaergic inputs from the intrinsic nuclei of the tectothalamic tract, namely the nucleus subpretectalis (Sp), the nucleus interstitio-pretecto-subpretectalis (IPS) and the nucleus posteroventralis thalami (PV) (Tombol et al., 1994; Mpodozis et al., 1996). Rt is located in the dorsal anterior thalamus, and in coronal sections appears as a round nucleus with a diameter of approximately 1 mm. We chose this nucleus to first test the solid microinjector because it is located deep in the pigeon brain, it is well delimited, and its input–output connections are well established. In addition, Rt is easy to identify electrophysiologically, since most of its neurons respond vigorously to small moving dots of light presented almost anywhere in the visual field (Wang et al., 1993).

Five microinjections of DiI, in an equal number of animals, were aimed at Rt, under continuous electrophysiological recording. The crystals were ejected in the middle of zones in which neural responses to motion — of the kind typically found in Rt — were recorded. The length of the cylindrical pellets loaded in the Microinjector ranged from 80 to 150 μm. After a survival period that varied from 5 days to 3 weeks, the small DiI pellets were found, unfragmented, in or around the expected brain structures. In all five cases, the crystals were located at a depth that coincided with the depth at which they were ejected. Four were successfully located inside the nucleus, whereas one was located in its inferior-lateral margin. Fig. 2A–B shows unstained coronal sections under light microscopy with two of the injection sites. The injections feature a very similar pattern, with a central dark rectangular core, which corresponds in size and shape to the loaded cylindrical pellet, and a larger circular zone, between 400 and 700 μm, which corresponds to the diffusion of the DiI into the surrounding tissue. The nucleus borders were drawn on the photographs to show that in both injections the DiI crystal and the diffusion zone are mostly circumscribed within the nucleus. In all five injections, the diffusion zone was circular, with very delimited borders. Its size was related — as expected — to both the size of the loaded crystal and the duration of the survival period. For instance, Fig. 2B corresponds to an injection of a 150 μm pellet and a survival period of 2 weeks, whereas Fig. 2A corresponds to an injection of an 80 μm pellet and a 5 day survival period.

When the sections were observed under epifluorescent illumination, the diffusion zone was highlighted, but its appearance and size did not significantly change. Nissl counterstained sections revealed that the diffusion zone is surrounded by a dense layer of macrophages, which are themselves filled with DiI. They may contribute to restrict the extent of the DiI diffusion by encircling the borders of the diffusion zone. Outside this zone, apparently healthy tissue with normal-looking neurons was observed.

As a result of the crystal injections of DiI into Rt, there was extensive retrograde labeling of neurons in most of the nuclei known to contain rotundal afferents. Conversely, no cell labeling was found in other nuclei not previously reported to contribute rotundal afferents, indicating that the injections were restricted and specific. In the five injections, retrograde labeled cells were found in the ipsilateral SP and PV and bilaterally in layer 13 of the optic tectum. Fig. 2C–D shows, for the injection presented in Fig. 2A, examples of DiI retrograde labeled cells in the ipsilateral SP and tectal layer 13. Since the projections of SP and tectal layer 13 upon Rt do not observe a point to point topography

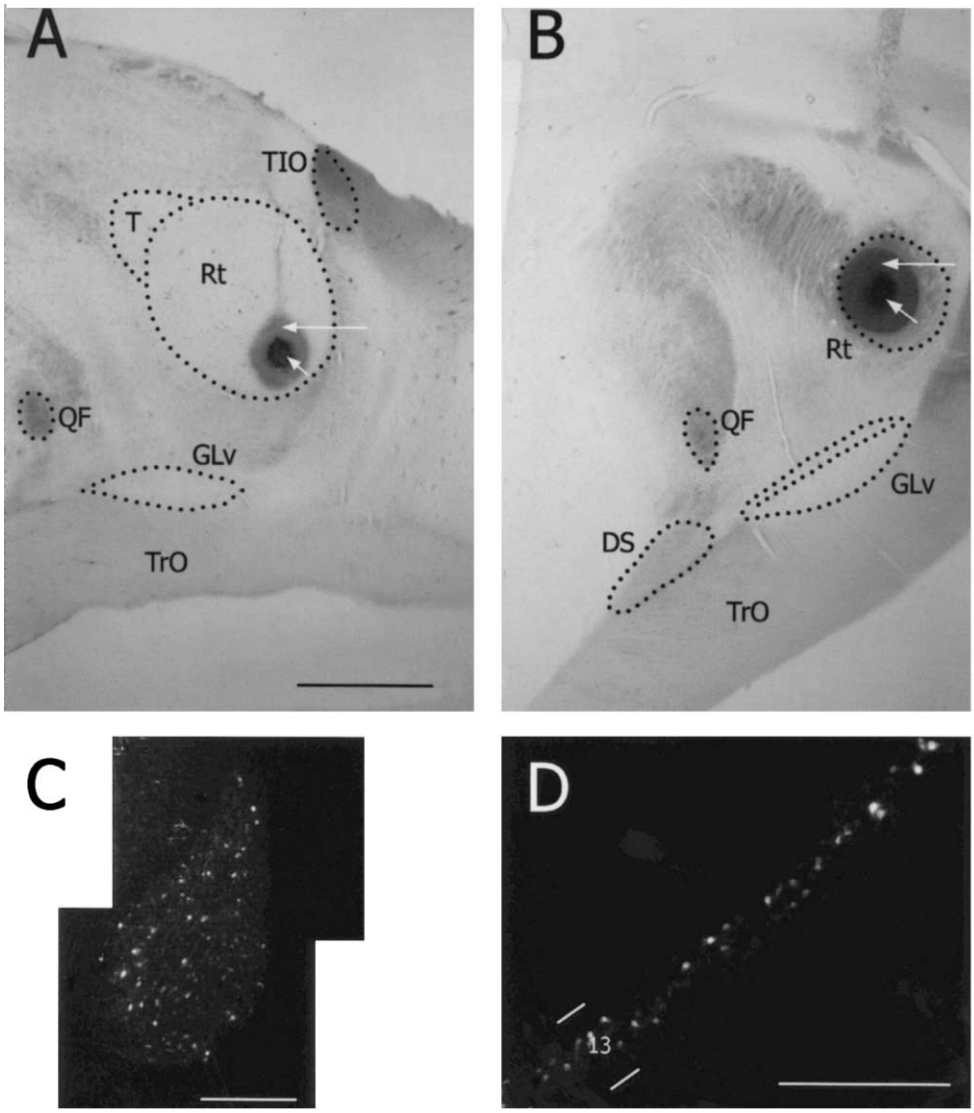


Fig. 2. Injections of DiI crystals into the nucleus rotundus: (A) and (B) are microphotographs of unstained transverse sections showing two injection sites of crystalline DiI. Dotted lines show the outlines of Rt and other surrounding structures: the nucleus triangularis (T), the tractus isthmo-opticus (TIO), the tractus opticus (TRO), the ventral lateral geniculate nucleus (GLv), the tractus quintofrontalis (QF), the dorsal supraoptic decussation (DS). Injection B is located at a more rostral level than injection A. In both cases the injections appear confined to Rt. The injection sites feature a dense central, rectangular core (short arrows), which corresponds to the injected crystal, and an external, well-defined circular diffusion zone (long arrows); (C) Retrograde fluorescent label of the nucleus subpretectalis resulting from the injection shown in A. The ventral pretectal area is shown. The nucleus is clearly outlined by the intensely retrogradely labeled neurons it contains; (D) Retrograde fluorescent label of the optic tectum after the same injection. The ventro-medial tectum, at the tegmental level, is shown. The fluorescent labeled cells are restricted to layer 13. Scale bar is 1 mm in A (also applies to B) and 500 μm in C and D.

(Karten et al., 1997), the labeled cells were distributed throughout the extension of these structures. In general the labeling was confined to the cell bodies and the proximal axon and dendrites, but we found some neurons in tectal layer 13 having long dendritic processes ramifying in layer 5, as has previously been reported (Luksch et al., 1998). Unlike the retrograde transport, anterograde DiI transport from Rt to the ectostriatum was less intense. Under epifluorescent illumination, the ectostriatum fluoresced above background, indicating that the DiI was transported, but no discernible fibers or terminals were observed.

Although a tenuous fluorescent tract usually marked the trajectory left by the instrument, no DiI fragments were observed on that tract, indicating that the crystal is adequately held inside the tip. The fluorescent tract was almost certainly produced during the withdrawal of the instrument, after the crystal was released, because it was not observed in penetrations where the crystal was not ejected. No significant neural transport was originated from the tract, since the afferents to the structures crossed by the tract (for example, the nucleus opticus principalis thalami, OPT, in the penetrations to

Rt, or Rt itself in the penetrations to the ventral lateral geniculate nucleus, see below) were never labeled.

### 3.2. DiI injections into the ventral lateral geniculate nucleus

Because of its deep location on the floor of the thalamus, just above the optic tract, the ventral lateral geniculate nucleus (GLv) represented a good target to test the microinjector. The GLv has a relatively simple laminar structure, with a lamina interna defined by a densely packed layer of cell bodies, which gives rise to the descending projection of the nucleus. The lamina externa or neuropil, contains interneurons, radially oriented dendritic arbors of the projection cells, and the terminal ramifications of incoming axons from the retina, tectal layer 10, nucleus lentiformis mescencephali pars magnocelularis (LMmc), the ventolateral thalamus (VLT) and the visual wulst (Crossland and Uchwat, 1979; Medina and Reiner, 1994; Shimizu et al., 1994; Karten and Mpodozis, unpublished results).

Electrophysiologically, the GLv has a clear signature. As the microelectrode approaches the nucleus, a brisk evoked negative wave in response to the onset of light is recorded above the lamina interna and throughout the GLv depth (author's unpublished results). Also, in and around the lamina interna, characteristic color-specific sustained discharges are recorded (Author's unpublished results; Maturana and Varela, 1982). We used this specific property to assess the precision of the method to deposit the crystal at an electrophysiologically identified position.

Fig. 3A shows PSTHs of a typical response, recorded around the internal lamina of the GLv, to monochromatic light projected on its receptive field. The response has a clear color preference, with a strong ON discharge to blue and green, and a reduced response to colors of longer wavelength. The DiI crystal was delivered at this recorded location. Fig. 3B shows a coronal section through the thalamus with the resultant injection site. The center of the DiI crystal clearly intersects the outlined GLv lamina interna. In this case the loaded crystal was $80 \times 150$ μm and the survival period was 2 weeks. Accordingly, the central rectangular core of the injection is small but the diffusion zone (approximately 500 μm) is relatively large. Otherwise the general appearance of the injection site is identical to the ones presented above. Many retrogradely DiI-labeled cells were observed in the LMc and PPC nuclei (Fig. 3C), with well filled cell bodies and proximal dendrites and axons. Only scattered labeled cells were found in layer 10 of the optic tectum, probably because the DiI did not diffuse enough into the outer layer where the tectal afferences terminate. The main downstream target of the Glv, the lateral pontine nuclei, was distinctively labeled with fluorescence, indicating anterograde transport (Fig. 3D).

### 3.3. Injection of rhodamine-isothiocyanate into the retina

Rhodamine is one of the most frequently used neuroanatomical tracers and is transported well in both anterograde and retrograde directions (Köbbert et al., 2000). It has been applied in the retina in an aqueous solution as well as in crystal form (Thanos and Bonhoefer, 1983, 1987). The ability to introduce localized injections into the retina is crucial in many anatomical and developmental studies dealing with the topographic projection of the retina to its several central targets. We made two injections of crystalline RITC into the retinas of two different pigeons. Fig. 4A shows a retinal flatmount with one of the RITC crystals inserted into the inferior nasal quadrant. The injection site is quite delimited and very small compared to the total surface of the retina. An enlarged picture of the injection site, taken under epifluorescent illumination (Fig. 4B), shows the sharp limits of the diffusion zone and a thin tract of labeled fibers emerging from the crystal. The tectal terminal field, also quite delimited, is shown in Fig. 4C, and matches the previously reported pattern of retino-tectal terminals in pigeons (Cowan et al., 1961). The terminal field extends from layer 2 to 7, and some individual fibers can be discerned. In the center of the terminal field, a small dark core, probably reflecting some fiber degeneration due to the crystal insertion, is observed. In addition, 10 cells were retrogradely labeled in the nucleus isthmo-opticus (IOn), which, in birds, is the source of centrifugal fibers to the retina (Cowan, 1970).

## 4. Discussion

The main achievement of the method we presented here is to facilitate the insertion of solid tracers into any structure in the brain that can be reached stereoataxically. Our experiments show that the method is highly reliable, and generally results in the accurate placement of the crystal pellets at the expected locations. This is confirmed both by the depth of the injection, which coincides with the readings of the micrometer, and by the electrophysiological signature at the injection point, which coincides with that of the injected structure. An additional advantage of the method is that the size of the load and its extrusion distance can be accurately controlled by simple adjustments on the microinjector at the moment of the loading process.

The use of the microinjector with DiI resulted in injections that, considering the outer ring of diffusion,

have a size comparable to that of the smallest injections of tracer solutions usually reported in the literature. However, the method has the advantage of producing cleaner and more well-defined injection sites, facilitating the interpretation of the results. Also, the results suggest that the effective area of injection, i.e. the area from which neural transport is originated, is smaller than the area limited by of the outer ring of diffusion. In effect, in the case of the GLv injection, the crystals are confined to the internal lamina of the nucleus, while the outer ring clearly reached the external lamina of the GLv. However the optic tectum showed only a few labeled cells in layer 10, indicating that the areas covered by the outer ring did not generate substantial transport. Thus, the effective area of injection appears to be restricted to the immediate vicinity of the DiI crystals. These observations are in agreement with other studies that have used injections of DiI crystals (Nakamura and O'Leary, 1989), and further contributes to the specificity of the results obtained with this method.

The injection of crystalline RITC into the retina also produced very restricted and clean injection sites. Such neat injection sites would be very difficult to attain with a pressure injection of diluted RITC. Furthermore, the results show the adequacy of the instrument for the insertion of dye crystals into retinal zones normally unreachable by a surgical deposition procedure. These characteristics are very valuable for studies aimed at visualizing the development of retinal axons

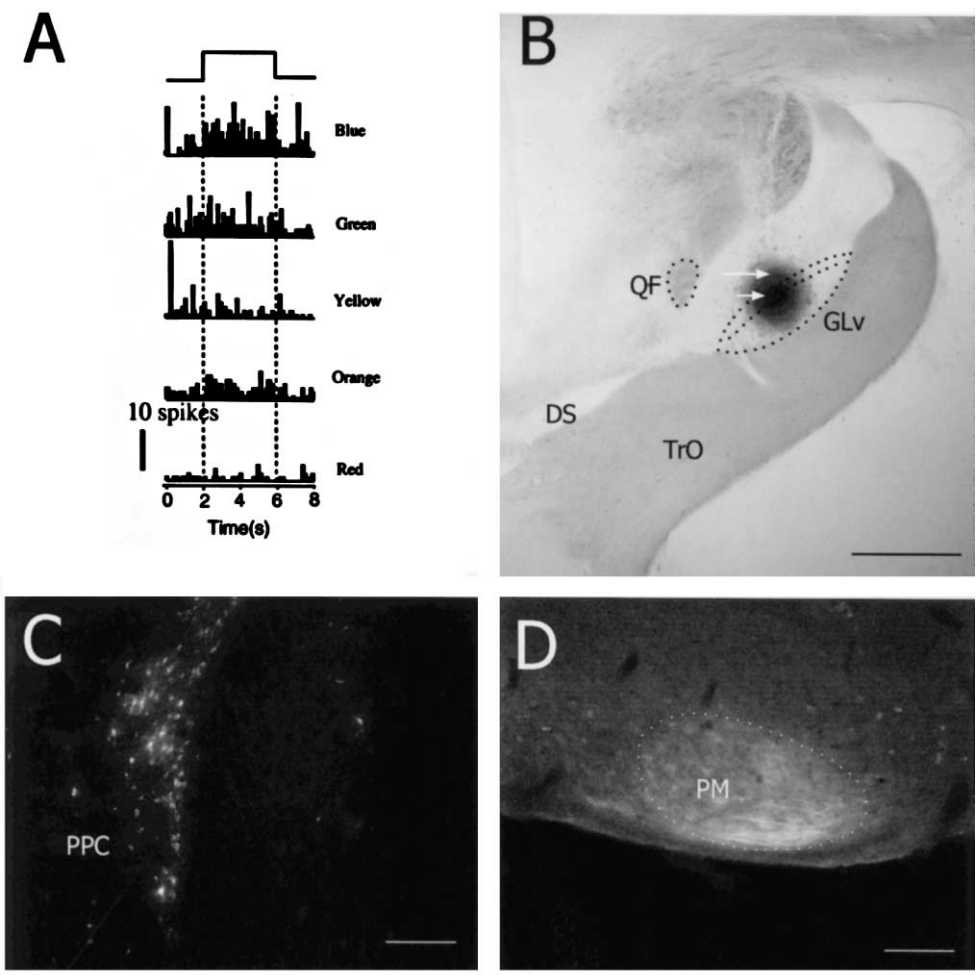


Fig. 3. Injection of a DiI crystal into the ventral lateral geniculate nucleus: (A) Peri-stimulus time histograms showing the chromatic responses of an isolated unit recorded at the site of the injection. Each histogram shows the activity of the unit before, during and after the illumination of its receptive field with a ganz field of light of different colors. The superior diagram and the vertical dotted lines indicate the onset and offset of the stimulus. Colors were calibrated for equal photonic flux. Note that the unit is preferentially excited by blue and green. In B, C and D microphotographs of unstained transverse sections are shown; (B) Injection site. The central core of the injection is located in the lamina externa of the nucleus (short arrow), while the circular diffusion zone (long arrow) extends to the internal lamina and to the surrounding ventro thalamic structures; (C) Retrograde fluorescent label of the nucleus pretectalis precomisuralis (PPC) after the injection shown in B. The medial pretectal area is shown. The nucleus is clearly outlined by the intensely retrograde-labeled neurons it contains; (D) Anterograde fluorescent label of the nucleus pons medialis (PM), after the same injection. The ventral pontine region is shown. A dense plexus of afferent processes confined to boundaries of the PM appears distinctively labeled. Scale bar is 1 mm in B and 200 μm in C and D.

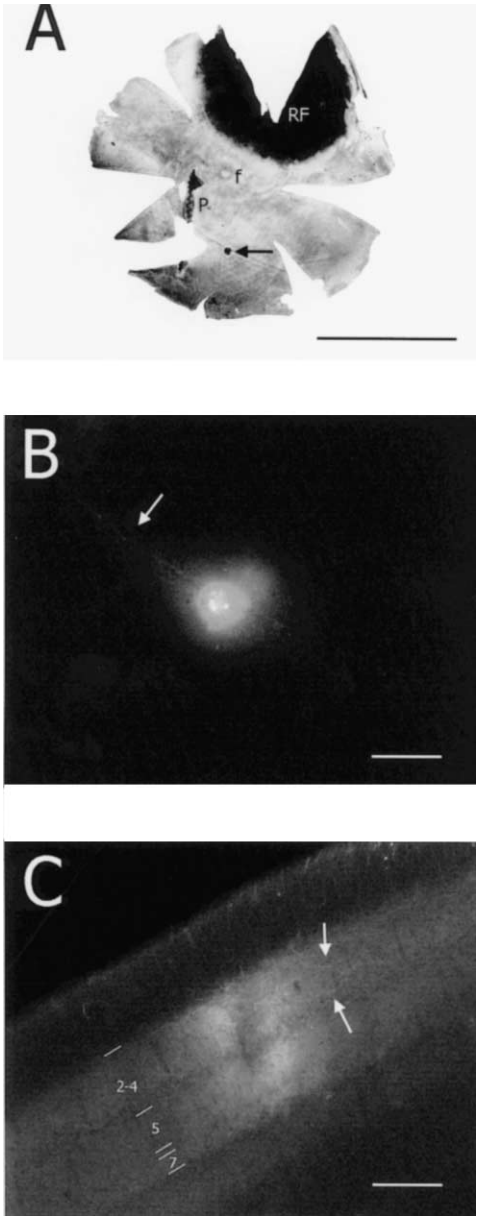


Fig. 4. Injection of an RITC crystal into the retina: (A) Photograph of a retinal flatmount showing a crystal of RITC (thin arrow) inserted into the inferior-nasal quadrant of the right retina of a pigeon. The red field (RF), the fovea (f) and the pecten (p) are marked as references: (B) Enlarged microphotograph of the injection site taken under epifluorescent illumination showing a thin bundle of fibers (arrow) emerging from the crystal in route to the optic nerve; (C) Terminal field of the fibers in the superior quadrant of the contralateral optic tectum. Arrows mark some individual axons. Numbers indicate the superficial tectal layers. Scale bar is 1 cm in A, 1 mm in B and 200 μm in C.

and the fine topographic connections between the retina and the rest of the brain.

Usually the instrument leaves a weak fluorescent tract when withdrawn, as the tip of the needle may get contaminated when the tracer is extruded. This is an unavoidable problem in most injection procedures. Yet, at least when using DiI, we found no significant neural transport originating from that tract.

The sudden pressure shock produced by the extrusion of the solid pellet into the brain may produce unwanted tissue damage, other than the obvious local damage and glial reaction produced by the intrusion of the pellet into the tissue. However, the simultaneous recording of local neural responses during the pellet release did not reveal overt damage. On the contrary, visual responses were usually recovered at the site of the injection as soon as the pressure pulses ended, a situation that, in our experience, is less frequent in iontophoretic or pressure injections of dissolved tracers.

The main cause of failure when using the microinjector is a tendency of the crystal to remain attached to the shaft after the ejection procedure. In fact, this problem caused two failures in our preliminary tests. When this failures occurred, most of the tracer was withdrawn with the needle, and tracer debris was deposited along the penetration tract. As described in the Section 2, this situation can be avoided by applying several pulses of pressure at the moment of injection.

In conclusion, the method presented here permits microinjection of solid tracers into deep structures of the brain in a controllable way. The use of this method to perform microinjections of the tracers DiI and RITC results in clean and well-defined small deposits of the tracer from which well-developed neural transport is specifically originated. Currently, we are performing injections of crystalline RITC as well as other tracers, like DiO, true blue and choleratoxin subunit b, in central structures, with very satisfactory results. Microinjections of solid tracers may be preferable to the conventional injections of tracer solutions when the location and the extension of the injection is critical.

## Acknowledgements

We thank Diane Greenstein for editorial assistance. We also thank Solano Henriquez and Cristian Acevedo for technical assistance. This research was supported by grant # 1990045 from the Chilean Scientific Council (CONICYT) to J.M.

## References

Bechmann Y, Nitsch R. Identification of phagocytic glial cells after lesion-induced anterograde degeneration using double-fluorescence labelling: combination of axonal tracing and lectin or immunostaining. Histochem Cell Biol 1997;107:391–7.

Benowitz LI, Karten HJ. Organization of the tectofugal visual pathway in the pigeon: a retrograde transport study. J Comp Neurol 1976;167:503–20.

Catsicas S, Thanos S, Clarke PGH. Major role for neuronal death during brain development: refinement of topographic connections in birds. Proc Natl Acad Sci USA 1987;84:8165–8.

Cowan WM. Centrifugal fibers to the avian retina. Br Med Bull 1970;26:112–7.

Cowan WM, Adamson L, Powell TPS. An experimental study of the avian visual system. J Anat (London) 1961;95:545–63.

Crossland WJ, Uchwat CJ. Topographic projections of the retina and optic tectum upon the ventral lateral geniculate nucleus in the chick. J Comp Neurol 1979;185:87–106.

Cruz F, Lima D, Coimbra A. Several morphological types of terminal arborizations of primary afferents in laminae I–II of the rat spinal cord, as shown after HRP labeling and Golgi impregnation. J Comp Neurol 1987;261:221–36.

Dietrichs E, Walberg F. The cerebellar nucleo-olivary and olivocerebellar nuclear projections in the cat as studied with anterograde and retrogade transport in the same animal after implantation of crystalline WGA-HRP. III. The interposed nuclei. Brain Res 1986;373:373–83.

Escher G, Schonenberg N, van der Loos H. Detergent-soaked HRP-chips: a new method for precise and effective delivery of small quantities of the tracer to nervous tissue. J Neurosc Methods 1983;9:87–94.

Griffin G, Watkins LR, Mayer DJ. HRP pellets and slow-release gels: two techniques for greater localization and sensitivity. Brain Res 1979;168:595–601.

Karten HJ, Hodos W. A Stereotaxic Atlas of the Brain of the Pigeon (*Columba livia*). Baltimore, MD: Jonhs Hopkins Press, 1967.

Karten HJ, Cox K, Mpodozis J. Two distinct populations of tectal neurons have unique connections within the retinotectorotundal pathway of the pigeon (*Columba livia*). J Comp Neurol 1997;387:449–65.

Keller F, Lipp HP, Waser PG. The organization of intrinsic hippocampal connections in explants of rat hippocampus studied by topical application of HRP crystals. Brain Res 1986;380:191–5.

Köbbert C, Apps R, Bechmann I, Lanciego JL, Mey J, Thanos S. Current concepts in neuroanatomical tracing. Prog Neurobiol 2000;62:327–51.

Luksch H, Cox K, Karten HJ. Bottlebrush dendritic endings and large dendritic fields: motion detecting neurons in the tectofugal pathway. J Comp Neurol 1998;396:399–414.

Maturana H, Varela F. Color-opponent responses in the avian lateral geniculate nucleus: a study in the Quail (*Coturnix Japonica*). Brain Res 1982;247:227–41.

Medina L, Reiner A. Distribution of cholyne acetyltransferase immunoreactivity in the pigeon brain. J Comp Neurol 1994;342:497–537.

Mpodozis J, Bischof H, Cox K, Shimuzu T, Woodson W, Karten HJ. Gabaergic input to the nucleus rotundus (*pulvinar caudale*) in pigeons. J Comp Neurol 1996;374:204–22.

Nakamura H, O'Leary DDM. Inaccuracies in initial growth and arborization of chick retinotectal axons followed by course corrections and axon remodeling to develop topographic order. J Neurosci 1989;9:3376–795.

Novikova L, Novikov L, Kellerth JO. Persistent neuronal labelling by retrograde fluorescent tracers: a comparison between fast blue, fluoro gold and various dextran conjugates. J Neurosci Methods 1997;74:9–15.

Shimizu T, Cox K, Karten HJ, Britto LRG. Cholera toxin mapping of retinal projections in pigeons (*Columbia livia*), with emphasis on retino-hypothalamic connections. Vis Neurosci 1994;11:441–6.

Tamamaki N, Fujimori KE, Rumiko T. Origin and route of tangentially migrating neurons in the developing neocortical intermediate zone. J Neurosci 1997;17:8313–23.

Thanos S, Bonhoefer F. Investigation on development and topographic order of retinotectal axons: anterograde and retrograde staining of axons and their perikarya with rhodamine in vivo. J Comp Neurol 1983;219:420–30.

Thanos S, Bonhoefer F. Axonal arborization in the developing chick retinotectal system. J Comp Neurol 1987;261:155–64.

Thanos S, Seeger J, Kazca J, Mey J. Old dyes for new scopes: the phagocytosis-dependent long-term fluorescence labelling of microglial cells in vivo. Trends Neurosci 1994;17:177–82.

Tombol T, Egedi G, Nemeth A. Phaseolus vulgaris lectin labeled and GABA immunogold stained terminals in nucleus rotundus: an EM study. J Hirnoforsch 1994;35:233–52.

Wang YC, Jiang S, Frost BJ. Visual processing in pigeon nucleus rotundus: luminance, color, motion and looming subdivisions. Vis Neurosci 1993;10:21–30.